


Enhanced hyporheic exchange flow around woody debris does not increase nitrate reduction in a sandy streambed

Felicity Shelley  · Megan Klaar · Stefan Krause · Mark Trimmer

Received: 28 February 2017 / Accepted: 7 November 2017 / Published online: 22 November 2017
© The Author(s) 2017. This article is an open access publication

Abstract Anthropogenic nitrogen pollution is a critical problem in freshwaters. Although riverbeds are known to attenuate nitrate, it is not known if large woody debris (LWD) can increase this ecosystem service through enhanced hyporheic exchange and streambed residence time. Over a year, we monitored the surface water and pore water chemistry at 200 points along a ~ 50 m reach of a lowland sandy stream with three natural LWD structures. We directly injected ^{15}N -nitrate at 108 locations within the top 1.5 m of the streambed to quantify in situ denitrification, anammox and dissimilatory nitrate reduction to

ammonia, which, on average, contributed 85, 10 and 5% of total nitrate reduction, respectively. Total nitrate reducing activity ranged from 0 to $16 \mu\text{M h}^{-1}$ and was highest in the top 30 cm of the stream bed. Depth, ambient nitrate and water residence time explained 44% of the observed variation in nitrate reduction; fastest rates were associated with slow flow and shallow depths. In autumn, when the river was in spate, nitrate reduction (in situ and laboratory measures) was enhanced around the LWD compared with non-woody areas, but this was not seen in the spring and summer. Overall, there was no significant effect of LWD on nitrate reduction rates in surrounding streambed sediments, but higher pore water nitrate concentrations and shorter residence times, close to LWD, indicated enhanced delivery of surface water into the streambed under high flow. When hyporheic exchange is too strong, overall nitrate reduction is inhibited due to short flow-paths and associated high oxygen concentrations.

Responsible Editor: Jacques C. Finlay.

Electronic supplementary material The online version of this article (<https://doi.org/10.1007/s10533-017-0401-2>) contains supplementary material, which is available to authorized users.

F. Shelley (✉) · M. Trimmer (✉)
School of Biological and Chemical Sciences, Queen Mary
University of London, Mile End Road, London E1 4NS,
UK
e-mail: f.c.shelley@qmul.ac.uk

M. Trimmer
e-mail: m.trimmer@qmul.ac.uk

M. Klaar
School of Geography, University of Leeds, Leeds, UK

S. Krause
School of Geography, University of Birmingham,
Birmingham, UK

Keywords Anammox · Denitrification · Large woody debris · Nitrate · Riverbed · Restoration

Introduction

Anthropogenic manipulation of the nitrogen cycle, primarily through mineral fertilizer production (Haber–Bosch process) and the burning of fossil fuels, has more than doubled the annual input of fixed

nitrogen to the biosphere (Canfield et al. 2010; Gruber and Galloway 2008). Sustained population growth, and associated pressures on food and energy production, are likely to result in further unbalancing of this microbially-mediated macronutrient cycle (Godfray and Garnett 2014; Howden et al. 2013). Low nitrogen uptake efficiencies in agriculture [typically $\sim 50\%$ in the UK (Sylvester-Bradley and Kindred 2009)] mean that precipitation readily washes excess nitrogen from land into waterways. Although most fertilizer is applied as ammonium, the prevailing redox conditions in surface water allow the complete nitrification of ammonium to nitrate. This mass-delivery of nitrate to aquatic environments has already resulted in devastating ecological effects such as eutrophication (Carmargo and Alonso 2006; Erisman et al. 2013; McIsaac et al. 2001), as well as risks to human health (Powlson et al. 2008), and increased costs in the treatment of drinking water (Shrimali and Singh 2001).

Rivers play an important role in both the downstream transport and the mitigation of nitrogen pollution (Alexander et al. 2007; Seitzinger et al. 2002). An estimated 23% of the 150 Tg of the nitrogen applied by humans each year to land is washed directly into rivers (Schlesinger 2009). Low-order (headwater) streams are important in the downstream transport of diffuse nitrate (Alexander et al. 2007). However, rivers are not inert pipelines, on the contrary, they are actually biogeochemical hot spots (Benstead and Leigh 2012; McClain et al. 2003; Pinay et al. 2015), which also play a major role in the transformation of reactive nitrogen to less ecologically active forms (Bernhardt et al. 2005; Bernot and Dodds 2005). Across large catchments, nitrate attenuation is inversely correlated with stream-order, due to the relatively large surface area to volume ratios in smaller streams which aids surface water contact with the hypoxic bed (Alexander et al. 2000; Peterson et al. 2001). Efforts to reduce the downstream transport of nitrogen pollution should therefore focus on enhancing the biological removal of nitrate in low-order streams (Craig et al. 2008; Dodds and Oakes 2008; Filoso and Palmer 2011).

Despite increasing efforts to reduce excess nitrate delivery to rivers, loadings remain critically high across many agricultural and urban catchments (Bouraoui and Grizzetti 2011; Burt et al. 2008; Howarth 2008). Therefore, there is now increasing pressure to develop in-stream methods for tackling nitrate pollution. The reintroduction of large woody

debris (LWD) has become an integral part of many river restoration schemes world-wide and its impact on channel hydrological complexity, geomorphology and ecology have been evidenced in both field and experimental studies (Curran and Wohl 2003; Gippel 1995; Gurnell et al. 1995; Miller et al. 2010). LWD is known to enhance hyporheic exchange, through increased roughness (Kasahara et al. 2009), and there is increasing evidence of the importance of hyporheic flow-paths for nitrogen removal (Gomez-Velez et al. 2015; Krause et al. 2009, 2013). Further, LWD may also enhance nitrate removal as it encourages sediment accumulation and the decaying wood provides organic carbon (Krause et al. 2014). However, researchers are yet to examine the possible link between LWD in rivers and riverbed nitrogen removal in detail.

Previous attempts to determine the effect of LWD on nitrate attenuation (Aumen et al. 1990; Elozegi et al. 2016; Roberts et al. 2007; Warren et al. 2013; Webster et al. 2000) did not specifically measure nitrogen transformations within streambed sediments, but, instead, monitored downstream chloride and nitrate or ammonium concentrations following its release upstream of LWD structures. As such, these approaches provided first evidence of the potential net effect of LWD, without distinguishing between nitrate storage and transformation, and they were restricted in their spatial resolution. To properly determine whether LWD enhances the removal of nitrate from streams, high-resolution direct measurements of streambed nitrate processing are required to further elucidate previous reach-based assessments.

Here, we quantified nitrate reduction in a nitrate-rich sandy streambed rich in LWD. We combined *in situ* ^{15}N -nitrate tracer process measurements (Lansdown et al. 2014) with the analysis of detailed physiochemical streambed properties, and pore water residence times, to unravel the key drivers of nitrate attenuation around the LWD. We hypothesised that LWD would enhance hydrodynamic forcing of nitrate-rich surface water into the streambed through, for example, increased topographic heterogeneity (Krause et al. 2014). We expected sustained delivery of nitrate into hypoxic pore waters to encourage the growth of nitrate reducing bacteria, which should result in enhanced rates of nitrate reduction in the vicinity of streambed LWD structures. However, should LWD only induce shallow hydrodynamic

forcing, we hypothesise that very short residence times will actually inhibit nitrate reduction.

In contrast to many previous stream nitrogen cycle studies, we aimed to simultaneously quantify all three of the known routes for microbial nitrate reduction [here, total oxidised inorganic nitrogen ($\text{NO}_2^- + \text{NO}_3^-$): denitrification, anammox and dissimilatory nitrate reduction to ammonia. The push–pull technique for in situ measurement of nitrate reduction potential has been shown to give similar results to whole-reach ^{15}N -tracer experiments, but with the additional benefit of being able to tease out the relative contribution of the three possible nitrate-reducing processes (Lansdown et al. 2014). Denitrification has received most attention and is usually considered the dominant mode of reduction (Seitzinger 1988) but that may in part be due to the techniques applied that couldn't distinguish between all three modes (Lansdown et al. 2014, 2016). Anaerobic ammonium oxidation (anammox) is less widely reported in freshwater environments but has recently been shown to play a significant role in N_2 production in permeable sediments (Lansdown et al. 2016; Zhou et al. 2014). Anammox is performed by obligate anaerobic bacteria which use nitrite to oxidise ammonia to produce di-nitrogen gas (Van de Graaf et al. 1996), the stoichiometry of which actually makes it a more efficient sink for reactive nitrogen over denitrification (Lansdown et al. 2016; Thamdrup et al. 2006). Finally, dissimilatory nitrate reduction to ammonia (DNRA) conserves nitrogen within the biosphere by reducing nitrate to ammonium. Therefore, from a reactive nitrogen removal perspective, denitrification and anammox are preferable to DNRA. To maximise the removal of nitrate as it flows through a river, diversion of the flow into the carbon-rich and oxygen-depleted parts of the streambed is vital. Depending on the porosity, organic matter content and biogeochemical activity in the streambed, different flow-path lengths will be required in order for the nitrate to be fully reduced (Mulholland et al. 2008; Richardson et al. 2004; Trimmer et al. 2012; Zarnetske et al. 2011). In this sandy river we expected denitrification to be the dominant form of nitrate reduction, with lesser contributions for anammox and DNRA.

Methods

Field site

This study took place between September 2014 and October 2015 in a forested reach of the Hammer Stream, a sandy tributary of the River Rother in West Sussex, UK (Fig. 1). The catchment of the Hammer Stream covers 24.6 km² of agricultural (arable and pastoral) and forested land and the underlying geology is dominated by Greensands and Mudstones (British Geological Survey 2016) and it is a typical example of lowland rivers with elevated nitrate loading.

Ground penetrating radar (GPR) and sediment cores carried out for a parallel study (not presented here) showed that extensive clay lenses and peat layers at a depth of 1–2 m below the streambed effectively isolate the upper streambed in the reach used within this study from the underlying groundwater. Hyporheic flow is therefore dominated by down-welling surface water and bank flow contribution. The river banks are dominated by broadleaved deciduous trees which provide woody debris and leaf litter to the stream. Three prominent LWD structures were identified, each spanning > 50% of the channel width and causing visible depositional and erosional bed structures (Fig. 1). The several years old woody structures are natural and not part of any engineered restoration measures, and they were comprised of logs at least 1 m × 10 cm, as typically defines LWD (Keller and Swanson 1979).

Pore water and surface water sampling

Water level and temperature were measured using a pressure transducer (Levelogger 3001, Solinst, Ontario, Canada) and compensated for changes in atmospheric pressure changes using a barometer (Barologger Edge, Solinst, Ontario, Canada) installed in tandem at the site. Vertical head gradient measurements were obtained by standing the instream piezometers vertically for a minimum of 1 h prior to the use of a Solinst 102 M Mini Laser Marked Water Level Meter (Solinst, Georgetown, Ontario, Canada) to measure the height of the water level inside and on the outside of the piezometer tube relative to the top of the tube. Vertical hydraulic gradient (VHG) was calculated by subtracting the outside depth from the inside and dividing by the height from the top of the

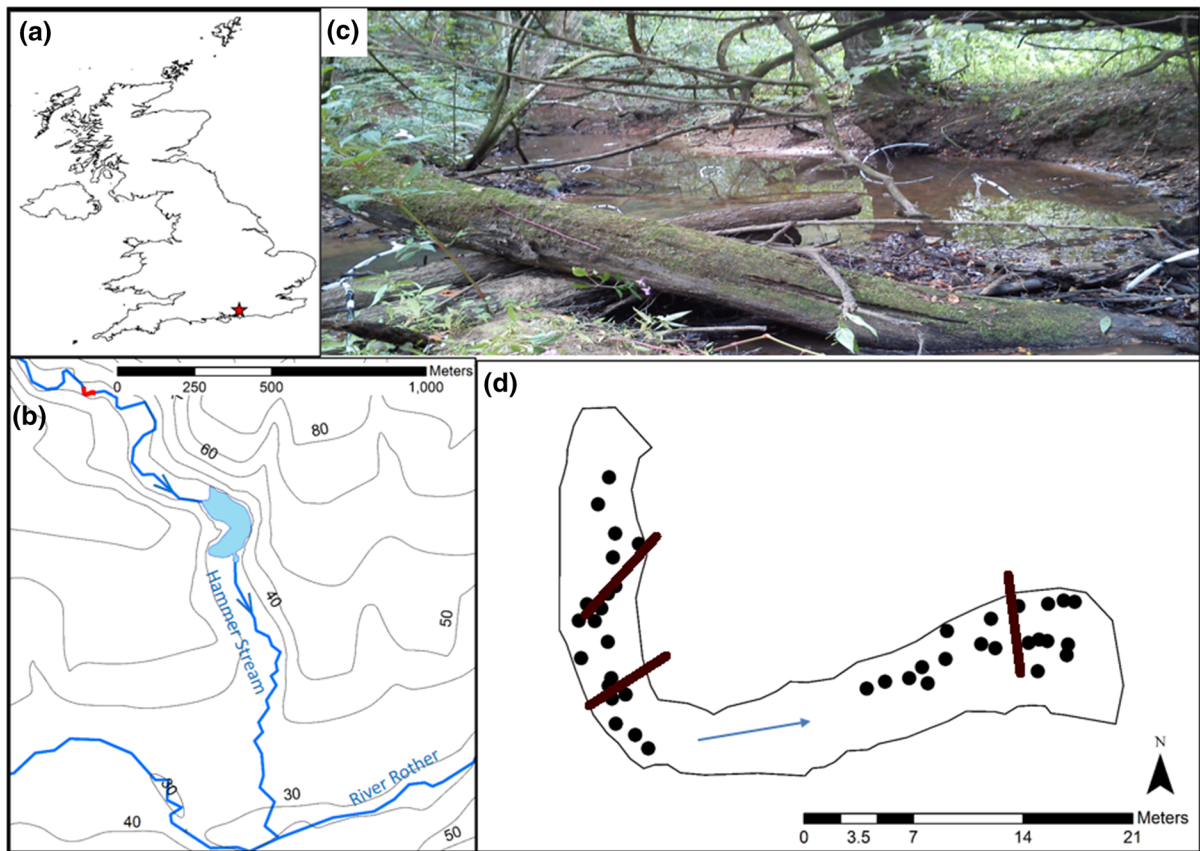


Fig. 1 Location and experimental overview of the study site **a** within the UK and **b** within the hilly forested catchment, upstream of the lake (study reach coloured in red); **c** a photograph of the most downstream LWD structure and newly installed flexible piezometer-sampling tube bundles, taken

facing upstream from a sandbar, under baseflow conditions (September 2014); **d** diagram of the 40 piezometer locations laid over the channel outline, with the LWD structures marked as brown lines. (Color figure online)

piezometer to the streambed. Data were collected each season at the same time as the nutrient sampling. VHG data for each piezometer and season were then plotted in ArcGIS (10.3.1; ESRI, Redlands, CA, USA) and an Inverse Distance Weighting applied to interpolate between individual points.

Porewater was sampled via multi-level mini-piezometers, comprising bundles of flexible Tygon tubing installed by hand at 40 locations along the reach (see Supplementary Fig. S1). Multi-level mini-piezometers, largely following the designs of Krause et al. (2013) and Rivett et al. (2008), consisting of a central flexible tube (length 2.5 m, internal diameter (i.d.) 12 mm) with five smaller (i.d. 2 mm) water sampling tubes, terminated with nylon filter material at 10, 20, 30, 50 and 100 cm within the streambed, affixed around its edge, giving us 200 sampling points

across a three-dimensional streambed array. During each campaign, the length of exposed tubing (above the sediment surface) was measured in order to adjust the “true depth” of the pore water sampling tubes which changed due to natural scour and deposition of sands.

Following installation in September 2014, week-long sampling campaigns were conducted four times over a year from November 2014 (in November, February, May and July), during which all 200 streambed points and the surface water were sampled for background chemistries. Afterwards, a subset of locations ($n = 76$) were targeted for in situ measures of potential nitrate reduction (Lansdown et al. 2014). The subset consisted of the shallowest depth (10 cm), at all 40 locations ($n = 40$), and then an additional 9 locations at all depths (3 in the upstream section, 3 in

the control reach, and 3 in the downstream section, $n = 36$). To maximise replication where tubes were either damaged or blocked, neighbouring depths were used instead.

To increase the spatial resolution around the two largest LWD structures in October 2015, a further 32 points in the streambed were investigated by installing stainless steel mini-probe samplers (Lansdown et al. 2014) to 15 cm into the bed (see Supplementary Fig. S1). The methods were carried out exactly as above to characterise the pore water chemistry and measure the potential for nitrate reduction in these additional locations.

The surface water was sampled mid-channel and mid-depth in the upstream ($n = 3$) and downstream ($n = 3$) sections, and pore water samples (10 mL) were withdrawn from the top of the sampling tubes using luer-lock sterile 12 mL syringes. To measure the ambient methane and nitrous oxide concentration, 3.5 mL of the sample was gently discharged into a 3 mL gas tight vial (Labco, Lampeter, UK) allowing to overflow slightly to minimise air contamination, before poisoning with ZnCl_2 (25 μL , 50% w/v) and capping. Next, oxygen, pH and temperature were measured using a calibrated fast-response glass oxygen electrode (OX50, Unisense, Aarhus, Denmark) and a field pH meter with a dual temperature and pH sensor (pH 100, VWR International, Radnor, USA). Finally, ~ 5 mL of the sample was filtered (0.45 μm polypropylene, Gilson Scientific, Luton, UK) into plastic tubes (polypropylene, VWR International) and frozen in a portable freezer until analysis. In May, extra samples were taken for iron (II) whereby 1.5 mL of sample was dispensed directly into a solution of buffered phenanthroline (3.5:1, pH 4.5 acetate buffer/0.2% (w/v) 1-10-phenanthroline monohydrate) for preservation awaiting further colorimetric analysis in the laboratory (Eaton et al. 2005).

Analytical methods for determination of gas and nutrient concentrations

Gas chromatography (GC) was used to determine the concentration of methane in the pore water. A helium headspace (1 mL) was introduced into each gas-tight vial and, after equilibration (> 2 h shaking), 50 μL of the headspace was withdrawn and injected into a GC fitted with a flame ionising detector (GC-FID) to measure CH_4 [Agilent Technology, UK, for full

specification see Sanders et al. (2007)]. The concentration in the original water sample was calculated using peak areas from a certified standard gas mixture (100 ppm CH_4 , Scientific and Technical Gases, UK) and appropriate solubility coefficients (Weiss and Price 1980; Yamamoto et al. 1976).

Using the filtered and frozen samples, the concentration of nitrite (limit of detection (LOD) 0.04 μM), nitrate (LOD 0.1 μM), ammonium (LOD 0.8 μM) and soluble reactive phosphorus (SRP, LOD 0.1 μM) was quantified using standard colorimetric methods (Kirkwood 1996), on an automatic segmented-flow analyser (Skalar, San++, De-Breda, Netherlands). Dissolved organic carbon (DOC) was measured in the filtered water samples using a total organic carbon analyser (TOC-VWP, Shimadzu, UK, LOD 50 μM). Iron (II) concentration was determined by absorbance at 520 nm on an ultraviolet/visible spectrophotometer (LOD 1 μM , precision 1%; Evolution 100, Thermo Fisher, USA).

Field methods for measuring in situ nitrate reduction

We used the isotope tracer “push–pull” technique previously described by Lansdown et al. (2014, 2016) to quantify the in situ potential for nitrate reduction to either to di-nitrogen gas (N_2) or ammonium (NH_4^+). We took a 10 mL sample of the pore water to characterise ambient pore water chemistries prior (< 20 min) to injecting tracers and re-measured all parameters detailed above. The tracer solution consisted of deoxygenated (10 min bubbling with oxygen-free nitrogen, BOC, UK) artificial river water (as in Lansdown et al. 2014 modified from Smart and Barko 1985) with 300 μM ^{15}N -nitrate (98 at.%, Sigma Aldrich, UK) as a reactive tracer, and 10 mM potassium chloride as a conservative tracer. We injected 28 mL of tracer (8.2 μmol of ^{15}N) at each location and then recovered 7 mL of the tracer/pore water mix after approximately 0, 10, 25 and 35 min. Following the recovery of each timed 7 mL sample, ~ 3.5 mL was discharged into a gas-tight vial and poisoned (as above) for ^{15}N - N_2 and ^{15}N - N_2O analysis, and the remaining sample was filtered (as above) and frozen for chloride and ^{15}N - NH_4 analysis.

Advective–dispersive flow of streambed pore water was estimated by calculating the dilution of the conservative tracer (KCl) over the duration of the

nitrate reduction measurements (~ 35 – 50 min) and the linear portion of the decay in chloride concentration was used to calculate a rate. The concentration of chloride was measured in the laboratory, using an ion-selective electrode (ISE Electrode, Cole Palmer, Stone, UK) which was calibrated against prepared standards (sodium chloride, 0–20 mM).

Laboratory determination of nitrate reducing potentials in sediment slurries

In addition to the in situ measurement of nitrate reduction described above, we also wanted to characterise the relative nitrate reducing potential of the sediments regardless of their in situ chemistry, under controlled laboratory conditions using sediment slurries. Surface sediments from the top 10 cm (< 15 cm horizontal distance from each piezometer bundle) were collected throughout the reach ($n = 3$) using a small plastic tub and then transferred into an anoxic glove-box (CV204, Belle Technology, Weymouth, UK). Following homogenisation, ~ 1 g wet sediment and 900 μL of nitrate-free artificial river water (Smart and Barko 1985) were added to gas-tight vials (3 mL). The sediment slurries were then left to “pre-incubate” for 24 h to reduce any traces of ambient ^{14}N -nitrate and oxygen before starting the ^{15}N experiments (Risgaard-Petersen et al. 2004). To start the experiment, 100 μL of 98 at.% ^{15}N -sodium nitrate was injected through the butyl septum of each vial ($n = 4$ per original sediment sample), then they were then gently shaken (rpm 60, SSM1 Orbital Shaker, Stuart, Stone, UK) before bacterial activity was stopped via injection of 100 μL of zinc chloride after 0, 1.5, 4 and 6 h (see Lansdown et al. 2012 for more detail). One vial for each original sediment sample was left to incubate without ^{15}N -sodium nitrate to serve as a reference measure of ^{15}N - N_2 natural abundance.

Analytical methods for determination of nitrate reduction

Here we wanted to test the effect of large woody debris on any in situ sediment potential to reduce nitrate directly within the stream bed. To do that we injected $^{15}\text{NO}_3^-$ at the same, non-rate-limiting concentration at each point in the bed and used the ^{15}N -labelling of recovered N_2 , N_2O and NH_4 pools, over time, relative to the reference samples, to calculate the in situ

potential rate of ^{15}N -nitrate reduction via denitrification, anammox and DNRA. The ^{15}N - N_2 content was determined by mass spectrometry. Calibration was performed using internal reference gas (analytical grade nitrogen, BOC, Guildford, UK) and N_2 in a helium headspace added to air-equilibrated water at 22 °C, run at the same time as the samples (Lansdown et al. 2014). An auto-sampler was used to inject 50 μL of the headspace into an elemental analyser interfaced with a continuous flow-isotope ratio mass spectrometer (Continuous Flow 20-22, Sercon Group, Crewe, UK), which measured the mass-charge ratios for m/z 28, 29 and 30 nitrogen ($^{28}\text{N}_2$, $^{29}\text{N}_2$ and $^{30}\text{N}_2$). To distinguish between ^{15}N - N_2 production via denitrification and anammox in situ, we used the ^{15}N labelling in any ^{15}N - N_2O production as a proxy for the ratio of $^{15}\text{NO}_3^-$ to $^{14}\text{NO}_3^-$ being reduced (Lansdown et al. 2016; Trimmer et al. 2006). N_2O was pre-concentrated prior to analysis by continuous flow isotope-ratio mass spectrometry (Precon, ThermoFinnigan, Ringoes, USA) and mass-charge ratios for 44, 45 and 46 were measured. For the sediment slurries, the ratio of $^{15}\text{NO}_3^-$ to $^{14}\text{NO}_3^-$ being reduced was simply equivalent to the ^{15}N at.% of the injected nitrate.

To quantify ^{15}N -DNRA, we performed a hypobromite oxidation of NH_3 to N_2 (after Risgaard-Petersen et al. 1995) on 1 mL of the recovered porewaters to quantify their ^{15}N - NH_4^+ content. Standards were prepared from ^{15}N - NH_4Cl (98 at.%, Sigma Aldrich) over a range of concentrations (5–600 μM) and isotope labelling (1–20%) similar to that expected in the samples. The concentration of total NH_3 (i.e. $^{14}\text{NH}_3$ plus $^{15}\text{NH}_3$ measured by segmented-flow colorimetric analysis, as above) was multiplied by the excess- ^{15}N - N_2 (relative to natural abundance) in the sample to give total ^{15}N - NH_4^+ and linear regression of this production against time was used to calculate a potential in situ rate of ^{15}N -DNRA.

We measured the production of $^{29}\text{N}_2$ as well as $^{30}\text{N}_2$ to calculate total $^{15}\text{N}_2$ production (denitrification + anammox), and the rate of either in situ or the sediment slurry activity was quantified using the following equation from Thamdrup and Dalsgaard (2000):

$$\Delta^x N_{2t=i} (nM N_2) = \left[\left(\frac{{}^x N_2}{\sum N_2} \right)_{t=i} - \left(\frac{{}^x N_2}{\sum N_2} \right)_{ambient} \right] \times \sum N_2 \times \alpha^{-1} \times V_s^{-1}, \tag{1}$$

where $\Delta^x N_2$ is the excess $^{29}N_2$ or $^{30}N_2$ in the sample at time i , ${}^x N_2 / \sum N_2$ is the proportion of $^{29}N_2$ or $^{30}N_2$ signal relative to the total signal ($\sum {}^{28}N_2 + {}^{29}N_2 + {}^{30}N_2$), α is the calibration factor (signal/nmol N_2), and V_s is the volume of sample in the vial (L). The in situ rates were then adjusted for advective flow using the chloride measurements and following equation adapted from Lansdown et al. (2014):

$$\Delta^{adjx} N_{2t=i} (nM N_2) = \Delta^x N_{2t=i} + \left[\left(\frac{[Cl^-]_{t=i} - [Cl^-]_{tracer}}{[Cl^-]_{ambient} - [Cl^-]_{tracer}} \right) \right] \times \Delta^x N_{2(t=i)}. \tag{2}$$

$\Delta^{adjx} N_2$ is the excess $^{29}N_2$ or $^{30}N_2$ in the sample at time i , corrected for any loss of $^{15}N-N_2$ or $^{15}NO_3^-$ tracer via advective flow within the streambed; $\Delta^x N_{2t=i}$ is the excess $^{29}N_2$ or $^{30}N_2$ calculated from Eq. (1) and Cl^- is the concentration of chloride in either the tracer solution (tracer), ambient pore water (background), or sampling time after the injection of the tracer ($t = i$). Following this adjustment, the rate of each process was calculated using linear regression of ^{15}N -produced against time.

To split total $^{15}N-N_2$ production into in situ potential rates of denitrification and anammox we used the ^{15}N labelling of N_2O produced (after Trimmer et al. 2006):

$$r_{14} N_2 O = \frac{\left(\frac{{}^{45} N_2 O}{\sum N_2 O} \right)_{sample} - \left(\frac{{}^{45} N_2 O}{\sum N_2 O} \right)_{ambient}}{2 \times \left[\left(\frac{{}^{46} N_2 O}{\sum N_2 O} \right)_{sample} - \left(\frac{{}^{46} N_2 O}{\sum N_2 O} \right)_{ambient} \right]}, \tag{3}$$

where ${}^{45}N_2O$ and ${}^{46}N_2O$ represent mass–charge ratios of 45 and 46, respectively, and $\sum N_2O$ is the sum of all three areas (${}^{44}+{}^{45}+{}^{46}N_2O$). We then compared the ^{15}N -labelling of the N_2O and N_2 produced in situ to calculate the contribution of anammox to total N_2 production as follows:

$$Q_{N_2O} = \frac{1}{1 + r_{14} N_2 O}, \tag{4}$$

$$contribution\ of\ anammox\ (\%) = \frac{2 - 2 \times \frac{Q_{N_2}}{Q_{N_2O}}}{2 - \frac{Q_{N_2}}{Q_{N_2O}}} \times 100, \tag{5}$$

where Q_{N_2} was calculated in the same way as Q_{N_2O} but using the production of $^{29}N_2$ and $^{30}N_2$ for $r_{14} N_2$, rather than ${}^{45}N_2O$ and ${}^{46}N_2O$, as was used for $r_{14} N_2O$. Subtracting the percentage contribution of anammox from total $^{15}N_2$ production gives the percentage contribution from denitrification.

The co-occurrence of DNRA and anammox could give rise to problems in calculating the relative contribution of each, due to the fact that DNRA will produce $^{15}N-NH_4^+$ which could then be oxidised through anammox with $^{15}NO_2^-$ (from the added $^{15}NO_3^-$) to also produce $^{30}N_2$ (A_{30}) in addition to that from denitrification (D_{30}). (see “Discussion” and Nicholls and Trimmer 2009).

Calculation residence times and Damköhler Numbers

We calculated water residence time from the conservative tracer data to assess if LWD-induced hydrological forcing affected the riverbed’s ability to reduce nitrate. Further we calculated the nitrate reaction time which allowed calculation of the Damköhler number (DaN) for each individual push–pull measurement. This is a unit-less ratio between the water residence time, and nitrate reaction time. We calculated water residence time as follow:

$$water\ residence\ time\ (h) = \left(\frac{1}{\Delta Cl^- / Cl_{MAX}^-} \right), \tag{6}$$

whereby ΔCl^- is the rate of decay of chloride (calculated by linear regression), our conservative tracer, and Cl_{MAX}^- is the maximum chloride concentration, at the beginning of the experiment. We then calculated the reaction time of the ambient nitrate pool, given the measured rates of ^{15}N -nitrate reduction as follows:

$$nitrate\ reaction\ time\ (h) = \left(\frac{1}{\Delta NO_3^- / NO_{3ambient}^-} \right). \tag{7}$$

Here, ΔNO_3^- is the rate of nitrate reduction (per litre of pore water) and $\text{NO}_3^-_{\text{ambient}}$ is the size of the nitrate pool in a litre of pore water. Thus, nitrate reaction time is the inverse of the nitrate turnover rate. Then, finally, we divided the water residence time by the nitrate reaction time as follows to give the unit-less Damköhler Number (DaN):

$$\text{Damkohler Number} = \frac{\text{water residence time (h)}}{\text{nitrate reaction time (h)}}. \quad (8)$$

When $\text{DaN} < 1$, the water is moving through the bed faster than the time taken for complete nitrate reduction (i.e. water residence time is shorter than the nitrate reaction time). Conversely, when $\text{DaN} > 1$, nitrate reduction exceeds water flux and so we would expect all of the nitrate present in the pore water to be completely reduced through denitrification, anammox and DNRA.

Statistical analyses

All statistical analyses were performed in the R software package (R Core Team 2015). Generalised mixed effects modelling was used to determine which physical and chemical drivers best explained the variation in measured nitrate reduction rate, which began by testing which of our random effects (month and piezometer) to include in the model. We first modelled the effect of each potential explanatory variable on nitrate reduction rate (log transformed) using a simple linear model. We then compared variations of each of these models in which we incorporated both month and piezometer location as a random effect on (i) the intercept only, (ii) the slope only and (iii) both the intercept and the slope (Bates et al. 2015). For each explanatory variable, we used a log-likelihood (ANOVA in R) approach to determine which model best explained variation in nitrate reduction rate (including or excluding random effects). Where there was no difference between the model with a random effect, and the simple linear model (ANOVA, $p > 0.05$) we concluded that the random effect did not significantly improve the fit of the model and it was therefore excluded from any further analysis. We then constructed a global linear mixed effects model which included temperature, ambient nitrate,

ambient oxygen, depth and residence time as fixed effects. We also tested for covariance between our fixed effects and found no issues of multi-collinearity i.e. all five variables added power to the model [variable inflation factor < 4 , “Car” package (Fox and Weisberg 2011)] and were therefore retained. Both month and piezometer were fitted as a random intercept. In addition, month was fitted as random effect on the slope of oxygen, whilst piezometer was fitted as random effect on the slope of ambient nitrate. All possible combinations of the global model terms were compared using the “dredge” function in the MuMIn package in R (Barton 2016) and we then used the small-sample corrected AIC (AICc) to determine the best fit model(s). Where the difference between a model’s AICc and the lowest AICc (i.e. ΔAICc) was < 2 , a set of best fit models was assumed and model averaging was used to identify the best predictor variables across the top candidate models and to determine their relative importance. Variable importance was calculated as the sum of the Akaike weights from all models in which they appear (Burnham and Anderson 2004).

Finally, to generate F -statistics and a significance level for each explanatory variable, we ran linear mixed effects models [R package nlme (Pinheiro et al. 2014)] for each variable, with the random effects included on the intercept, or slope and intercept (as above).

To test for differences in measured chemical variables and processes between locations in the LWD structures (< 1 m) and those away from the LWD (> 1 m), we performed a linear mixed effects model, with month and piezometer as random effects (intercept only), and we extracted the F and p values. The distance of 1 m from the LWD was chosen as a way of categorising the riverbed sampling positions as “in or very close to the LWD structures” or not. We acknowledge that the hydrological connectivity of the riverbed will vary across this reach, and while this may appear an arbitrary distance, our measures of vertical hydraulic gradient (see Fig. 2c) indicate that this is a reasonable distance to choose.

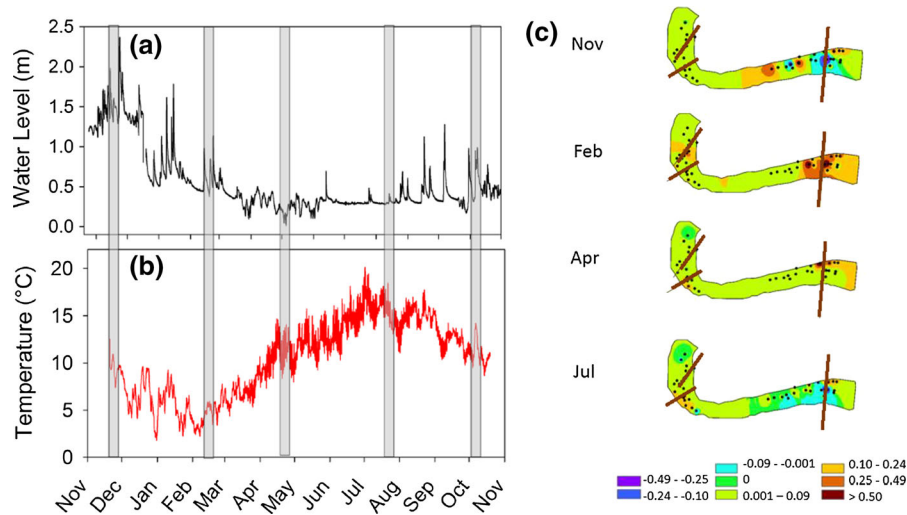


Fig. 2 Surface water **a** level above baseflow and **b** temperature, generated from 10 min interval data points, over the 12 month study period; **c** contour plots showing patterns in vertical hydraulic gradient across the network of 40 piezometers (depicted as black spots) spread along the study reach. The size and positioning of the three LWD structures are marked as brown lines and the colours represent strong positive head

(> 0.5 m, dark brown), through to neutral head (0 m, green) and negative head (0.5–0.8 m, lilac). Vertical grey bars on the first panels mark the five sampling periods with the first four when the vertical hydraulic gradient datasets were generated (i.e. main seasonal study), and the fifth grey bar marks when the additional work was carried out in October 2015 to increase resolution close to the LWD. (Color figure online)

Results

Seasonal site conditions

Surface water temperatures ranged from 2 to 20 °C and following a series of storm events, which increased water levels throughout the autumn and early winter (peak level 2.4 m above base flow), water levels dropped back towards base-flow, where they remained for spring and summer (Fig. 2). Water flowed over all three LWD structures when 1 m above base flow. Our sampling dates covered the entire range of water levels and temperatures measured in the stream (Fig. 2) which enabled us to test our hypotheses against a backdrop of natural variation.

Vertical hydraulic gradient (VHG) varied along the reach and the differences were most extreme in November and February (Fig. 2c) when the river level was high. Generally there was either no VHG or slightly gaining VHG around the top two LWD structures. But around the third and largest LWD structure (right of figures in 2c) the variation was extreme. In November when a flood forced flow over the downstream LWD and associated sandbar, there was intense (– 25 cm), localised (< 1 m) negative head and this was seen again in July but on a smaller

scale. Conversely, in February and April we measured strongly gaining VHG around this same structure (Fig. 2c).

Pore water chemistry

Pore water depth profiles showed that the surface water chemical signature did not penetrate below 30 cm (and much shallower in some locations) and that there was no discernible groundwater influence (Fig. 3). The sharp decrease in oxygen and nitrate concentration over the top 10 cm of riverbed, and simultaneous increase in ammonium, showed that the conditions were ideal for nitrate reduction. The high concentrations of ammonium, iron (II), organic carbon and methane in the riverbed indicated a strongly reducing environment (Table 1). Statistical analyses found that pH ($p < 0.0001$), nitrate ($p < 0.0001$), oxygen ($p < 0.012$), temperature ($p < 0.0001$) decreased with depth, and ammonium ($p < 0.003$) and methane ($p < 0.003$) increased with depth, and this relationship interacted with sampling month for pH and temperature (see Supplementary Table 1 for detailed results of all tests). There was no linear change in the concentration of soluble reactive phosphorous, organic carbon or iron (II) with depth

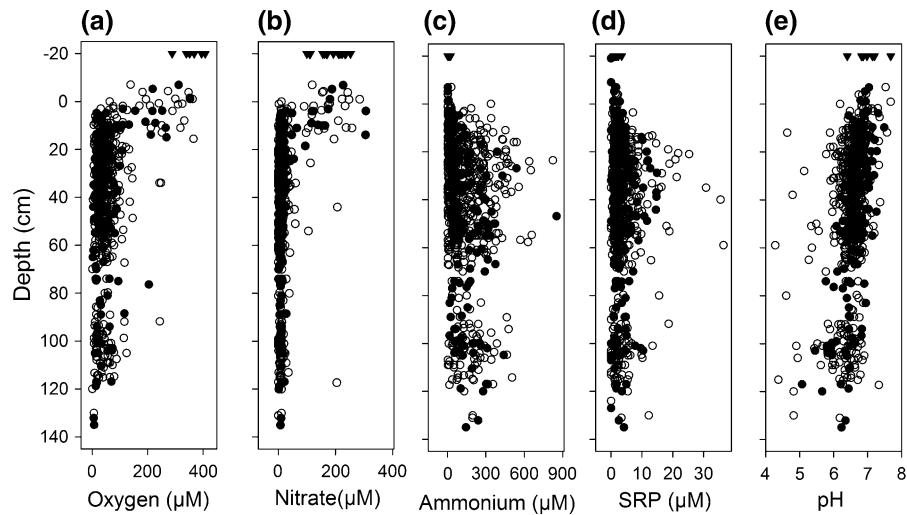


Fig. 3 Depth distribution of dissolved **a** oxygen, **b** nitrate, **c** ammonium, **d** soluble reactive phosphorous and **e** pH in the surface water (shown at -20 cm as filled triangles) and pore water. Points from within 1 m of LWD are shown in filled circles and those more than 1 m from LWD are shown in

unfilled circles. Depth was calculated on each trip by measuring the distance from the sediment surface to the top of the piezometer bundle to account for any scour or deposition since installation

Table 1 Background water chemistry in the surface water, shallow pore water and deep pore water

Variable	Surface water	Shallow sediment (0–30 cm)	Deep sediments (> 30 cm)
Dissolved oxygen (% sat.)	113.95	22.05	13.94
pH	6.97	6.68	6.46
Temperature ($^{\circ}\text{C}$)	13.22	12.59	12.76
Methane (μM)	5.61	392.73	525.19
Iron II (μM)	3.16	177.68	178.80
Nitrite (μM)	1.34	0.76	0.63
Nitrate (μM)	189.39	35.25	10.39
Ammonium (μM)	7.23	122.71	157.95
Soluble reactive phosphorous (μM)	1.46	3.54	3.63
DOC (μM)	320.43	734.30	742.39

Data shown are mean averages including data over the whole year. Depths are true depths at each sampling time, i.e. seasonal change due to scour and deposition has been accounted for

into the bed; although, all were higher in the bed, relative to the overlying surface water throughout the year (Table 1).

Streambed nitrate reduction

Denitrification, anammox and DNRA were all detected at 108 discrete in situ locations in all seasons and denitrification was the most dominant form of nitrate reduction (Fig. 4). Total nitrate reduction ranged from 0 to $16 \mu\text{M N h}^{-1}$ and the average

contribution via denitrification, anammox and DNRA was 85, 10 and 5%, respectively. Below 60 cm into the bed, nitrate reducing activity was consistently low ($< 1 \mu\text{M N h}^{-1}$), but in shallower sediments there was substantial variation (Fig. 4). Total nitrate reduction decreased significantly with depth ($F_{1,128} = 104$, $p < 0.0001$), as did denitrification ($F_{1,128} = 27$, $p < 0.0001$) and anammox ($F_{1,128} = 4.2$, $p = 0.04$), but DNRA did not ($F_{1,128} = 2.7$, $p = 0.104$). There was no difference in the rate of denitrification ($F_{1,67} = 1.6$, $p = 0.21$) or of DNRA ($F_{1,36} = 1.3$,

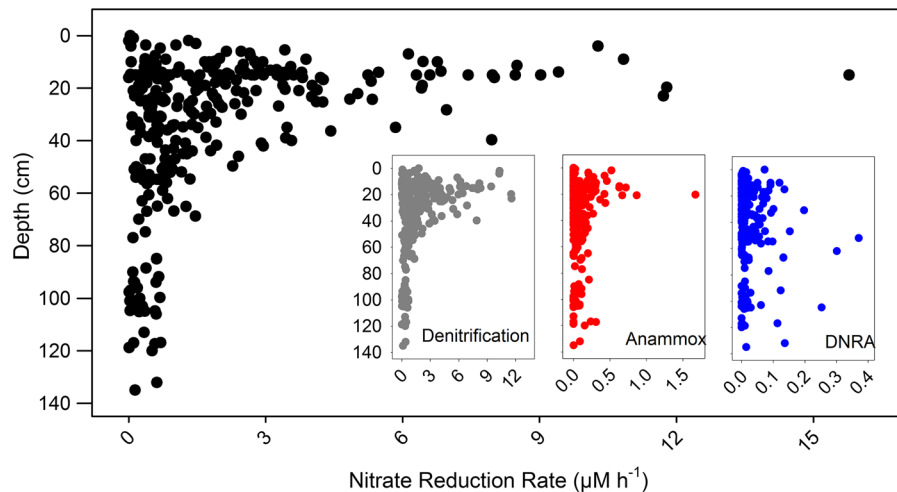


Fig. 4 Total nitrate ($^{15}\text{N}_2$, $^{15}\text{N}_2\text{O}$ and $^{15}\text{NH}_4^+$) reduction rate measured in situ at 76 locations (repeated each season), plotted against depth; inset, ^{15}N reduction via the three different pathways plotted against depth

$p = 0.27$) between locations < 1 m from LWD and those > 1 m from LWD. However, despite high variation, anammox was on average 77% faster close to the wood ($F_{1,67} = 4.2$, $p = 0.044$). Similarly, as a percentage of total nitrate reduction, significantly more was transformed via anammox around the LWD (12% vs. 8%, $F_{1,67} = 4.8$, $p = 0.03$), whereas there was no difference in the percentage attributed to denitrification ($F_{1,67} = 3.6$, $p = 0.06$) or to DNRA ($F_{1,36} = 0.32$, $p = 0.58$) as a function off wood.

We also used sediment slurries to measure the potential for denitrification and anammox in 35 surface sediment samples under controlled laboratory conditions. Total N_2 production ranged from $0.9 \text{ nmol g}^{-1} \text{ h}^{-1}$ to $11.0 \text{ nmol g}^{-1} \text{ h}^{-1}$, and averaged $2.7 \text{ nmol g}^{-1} \text{ h}^{-1}$. The percentage contribution from anammox ranged from 1 to 20% and averaged 9% with denitrification contributing 91% on average. DNRA was not quantified in these samples.

The effect of ambient temperature on nitrate reduction

Over the year, the pore water temperature ranged from 5 to 20 °C (average 12 °C) and, given the expected influence of temperature on metabolism, it was important to quantify its influence on our in situ estimates of nitrate reduction. Displaying the data on an Arrhenius plot (Fig. 5a) reveals a subtle temperature effect on total nitrate reduction (0.24 eV,

$F_{1,285} = 4.1$, $p = 0.045$). When broken down into the individual routes of nitrate reduction we found that both anammox (0.48 eV, $F_{1,212} = 13.1$, $p < 0.001$) and DNRA (0.56 eV, $F_{1,235} = 12.0$, $p < 0.001$) activity depended on temperature while denitrification did not ($F_{1,284} = 2.3$, $p = 0.13$, Fig. 4b). The variation around the regression lines shows that other environmental variables are causing differences in the nitrate reduction rate and temperature alone cannot explain the intra- or inter-seasonal variation.

Exploring the controls on nitrate reduction rate and potential effect of LWD

Nitrate reduction in situ was limited by short water residence times, and the peak in activity coincided with mid-range water residence times (~ 1 h, Fig. 6a). Residence time was significantly shorter around the LWD, relative to locations > 1 m from the LWD (Fig. 6b, Table 2, $F_{1,67} = 5.1$, $p = 0.027$), as indicated by faster rates of chloride decay following the tracer injection ($F_{1,67} = 8.5$, $p = 0.005$) which we attribute to greater hyporheic exchange. Around the LWD, the (surface) water depth was almost 3 times shallower than the rest of the reach, and methane concentrations were 11% lower (Table 2), adding weight to the idea of greater surface water downwelling closer to the wood where sand accumulates (greater bed heterogeneity). The VHG plots show this

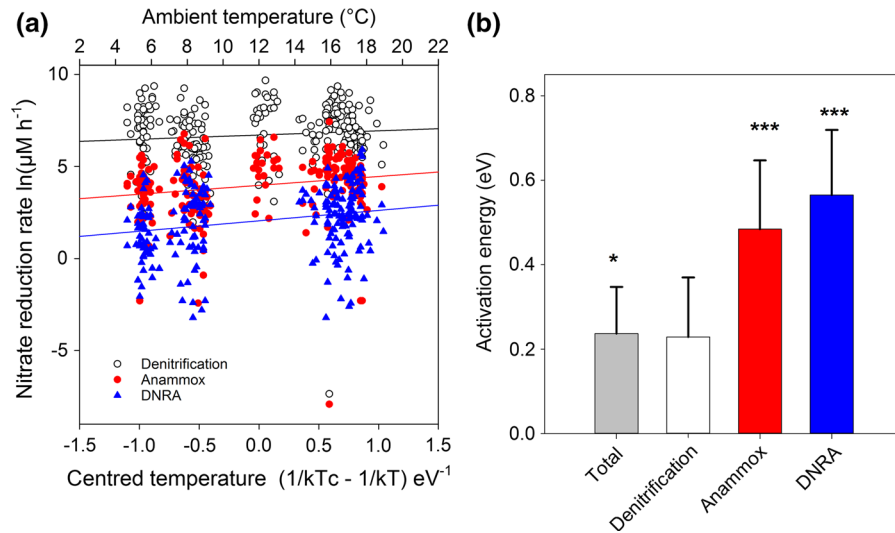


Fig. 5 The temperature dependency of nitrate reduction rates. **a** Arrhenius plot with centred temperature (where 0 is the mean average temperature) versus the natural logarithm of the three nitrate reduction processes. Unfilled circles are denitrification, red circles are anammox and blue triangles are DNRA. The slope of the regression line gives the activation energy. The black line is for total nitrate reduction, the red is for anammox,

hydraulic forcing is extremely localised around the LWD.

Nitrate reduction rate was highly variable when ambient nitrate was $< 40 \mu\text{M}$, but above this threshold, nitrate reduction was suppressed (Fig. 6c). This high nitrate is indicative of strong connectivity with the surface water and suggests redox conditions do not permit nitrate reduction. Further, there was 60% more nitrate in the pore water around the wood (Fig. 6d, Table 2), which also suggested greater surface water inputs. The non-linear, inverse correlation between ambient nitrate and nitrate reduction was much stronger in the sediment slurries in the laboratory (see inset, Fig. 6b). However, there was no interaction with this relationship and proximity to LWD ($F_{1,31} = 1.2$, $p = 0.29$), nor was there any difference in the nitrate reduction rates measured in the laboratory between sediments taken from around the LWD and those taken from further away ($F_{1,33} = 0.04$, $p = 0.84$).

Given the measured reduction rate and the ambient concentration, we calculated nitrate reaction time and found it was slower closer to the LWD (110 h vs. 29 h, $F_{1,67} = 4.1$, $p = 0.047$). Damköhler numbers collapse water residence time and nitrate reaction time into a

unit-less ratio, and Fig. 6e shows this data on a scatter plot. Although there was an inverse relationship between the two parameters (shorter water residence times associated with longer nitrate reaction times), there was no difference as a function of wood (Table 2). Similarly, there was no difference in the overall rate of nitrate reduction as a function of proximity to LWD (Table 2, Fig. 6f).

We constructed a global linear mixed-effects model to identify which variables best explained variation in the in situ rate of nitrate reduction and to determine their relative importance. The best fit model explained 44% of the variation (adjusted- R^2) in nitrate reduction rates (log transformed), and included depth, nitrate concentration and water residence time, as fixed variables, with month (repeat measures) and location within the reach (piezometer) included as random effects (see “Methods”). Three other candidate models, which displayed similar explanatory power included either temperature, oxygen or both, whilst retaining nitrate concentration, depth and water residence time, suggesting that these were the most important variables for explaining the observed variation in nitrate reduction rate (Supplementary Table 2). Individually ranked by explanatory power,

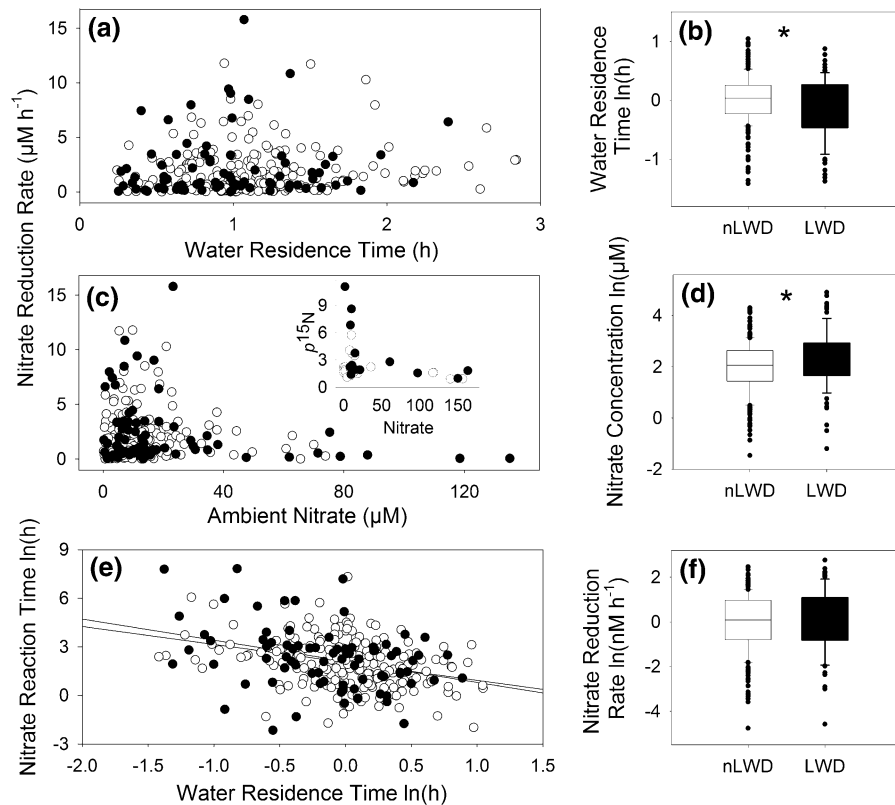


Fig. 6 **a** The rate of nitrate as a function of water residence time; **b** a boxplot showing the difference in water residence as a function of proximity to LWD; **c** nitrate reduction rate as a function of ambient nitrate concentration (main panel shows in situ push–pull measures ($\mu\text{M h}^{-1}$) and inset panel shows potential measures in the laboratory ($\text{nmol g}^{-1} \text{h}^{-1}$); **d** boxplot showing the difference in ambient nitrate with LWD proximity; **e** comparison of water residence time and nitrate reaction time

which form the Damköhler number; **f** boxplot showing the comparative spread of in situ nitrate reduction rate. Filled circles or boxes are always points in the riverbed < 1 m from one of the LWD structures and those > 1 m from the LWD structures are unfilled (white). Where the data are significantly different ($p < 0.05$), considering random effects of date and repeat measures, an asterisk is placed above the boxes

depth ($F_{1,128} = 104$, $p < 0.0001$) explained the most variation, followed by oxygen ($F_{1,128} = 5$, $p = 0.029$), temperature ($F_{1,128} = 5$, $p = 0.035$), water residence time ($F_{1,128} = 4$, $p = 0.063$) and finally ambient nitrate ($F_{1,128} = 2$, $p = 0.14$).

Mapping nitrate reduction over a woody streambed

Finally, we mapped our nitrate reducing activity data spatially in relation to the position of the LWD. The variation in water level (see Fig. 2), indicated that the hyporheic exchange flow likely varied across the year; we therefore mapped and analysed each season separately to tease out any effect of season on nitrate reduction in the shallow sediments (top 20 cm). We

overlaid the nitrate reduction data on a channel map, with the size and the orientation of all three LWD structures indicated, to examine the interaction between the three (see Fig. 7 and Supplementary Fig. S2).

In no individual seasons was nitrate reduction rate significantly faster around the LWD (Supplementary Fig. S2). However, in February, the concentration of pore water nitrate ($F_{1,28} = 6.1$, $p = 0.02$) was 188% higher around the LWD, and residence time was 39% shorter ($F_{1,28} = 5.7$, $p = 0.02$), indicating enhanced hyporheic exchange. However this difference was not significant in any other month. Although average nitrate concentration and nitrate reduction rate was generally higher around the LWD, due to small sample

Table 2 Mean averages concentrations for riverbed locations within 1 m of LWD and > 1 m from LWD

Explanatory variable	Average < 1 m from LWD	Average > 1 m from LWD	Model output
Dissolved oxygen (μM)	36.6	31.3	$F_{(1,67)} = 2.8, p = 0.097$
pH	6.6	6.6	$F_{(1,67)} = 0.02, p = 0.89$
Temperature ($^{\circ}\text{C}$)	12.2	12.0	$F_{(1,67)} = 0.0006, p = 0.97$
Nitrate (μM)	18.9	11.4	$F_{(1,67)} = 7.9, p = \mathbf{0.007}$
Ammonium (μM)	156.6	164.3	$F_{(1,67)} = 2.0, p = 0.16$
Phosphate (μM)	3.1	3.2	$F_{(1,67)} = 0.46, p = 0.50$
Methane (μM)	467.6	522.3	$F_{(1,67)} = 4.1, p = \mathbf{0.048}$
Organic carbon (μM)	817	1025	$F_{(1,67)} = 2.3, p = 0.14$
Water depth (cm)	14.6	40.6	$F_{(1,67)} = 76.4, p < \mathbf{0.0001}$
Residence time (h)	0.97	1.10	$F_{(1,67)} = 4.8, p = \mathbf{0.032}$
Total nitrate reduction ($\mu\text{M h}^{-1}$)	2.24	1.84	$F_{(1,67)} = 0.01, p = 0.94$
Denitrification ($\mu\text{M h}^{-1}$)	2.08	1.75	$F_{(1,67)} = 1.6, p = 0.21$
Anammox ($\mu\text{M h}^{-1}$)	0.13	0.08	$F_{(1,67)} = 4.2, p = \mathbf{0.04}$
DNRA (nM h^{-1})	34.7	20.6	$F_{(1,47)} = 3.7, p = 0.061$
Damköhler Number	0.48	0.50	$F_{(1,77)} = 2.7, p = 0.107$

Statistical model output for testing whether measured chemistry and processes differ as a function of proximity to a LWD structure. We used linear mixed effects models and fitted month, piezometer location and depth as random effects and where necessary the data were log-transformed. Where the difference is significant ($p < 0.05$) p -values are in bold

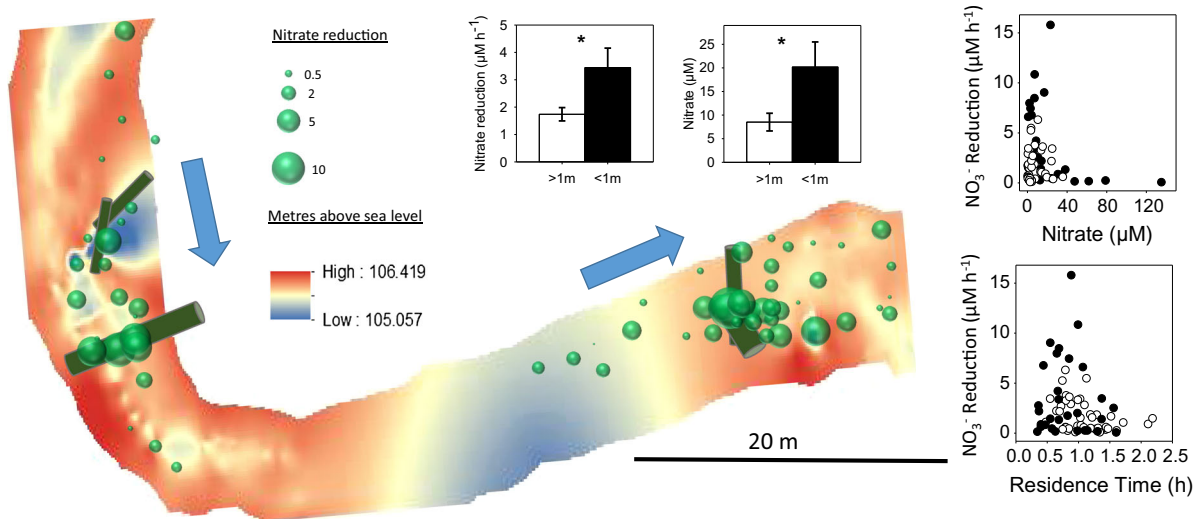


Fig. 7 Bubble plot showing the magnitude of measured nitrate reduction in the top 15 cm across the study reach in autumn (November 2014 and October 2015). Bubble size is proportional to nitrate reduction ($\mu\text{M h}^{-1}$), the relative size and orientation of large woody debris is depicted by brown cylinders and the direction of flow is indicated by the blue arrows. This plot is overlaid on top of a bathymetric contour plot. Inset (top) bar-

size particularly close to the LWD ($n = 8-11$), and the bi-modal spread of data (see Fig. 7) this difference was rarely statistically different.

charts to show the average nitrate reduction and ambient nitrate concentration in these shallow pore waters. Inset (right) scatterplots show the relationships between nitrate reduction rates, ambient nitrate concentration and residence time of the shallow pore water, both within 1 m of the wood (black symbols) and further away (white symbols)

The October dataset was acquired to increase our sample size close to the LWD and pooling these data with the November data from the previous autumn

gave us more statistical power (Fig. 7). With these pooled data, pore water nitrate concentrations were higher (137%, $F_{1,71} = 5.6$, $p = 0.021$), residence times were shorter (32%, $F_{1,70} = 8.6$, $p = 0.005$), and nitrate reduction rates were faster (98%, $F_{1,69} = 6.3$, $p = 0.014$), around the LWD, than in non-woody streambed locations.

Discussion

To the best of our knowledge, this study is the first to simultaneously quantify in situ the effects of LWD on denitrification, anammox and DNRA activity in streambed sediments. By measuring a whole suite of physiochemical variables in the background pore water before each of our isotope-tracer experiments, we were able to align the measures of nitrate reduction with a detailed chemical picture of the in situ streambed pore water matrix to help address our hypotheses.

Quantifying nitrate reduction in a sandy streambed and net organic mineralisation

The pore water chemistry data confirmed that streambed pore water conditions at the field site were ideal for nitrate reduction. Low pore water oxygen and nitrate, coupled with high ammonium were found to correlate with high rates of nitrate reduction as found in other streambeds (Krause et al. 2013; Lansdown et al. 2014; Zarnetske et al. 2011) and where we know there is hyporheic exchange, low pore water nitrate (relative to surface water), indicates that the bed is a likely a nitrate sink. The total rate of nitrate reduction recorded in our study was up to ten times higher than that which Lansdown et al. (2014) measured in the River Leith, a sandstone river with larger grain size than at the Hammer Stream. This is largely because the surface water-pore water gradients in oxygen and nitrate are much stronger in the more reduced, low-permeability fine-sand streambed sediments of the Hammer Stream (this study), compared to the far more permeable gravel/cobbled substrate at the Leith.

As hypothesised, denitrification was responsible for the bulk of in situ nitrate reduction in the Hammer Stream (average 85%), although anammox and DNRA were also quantified, and the calculated contribution of anammox was consistent between the in situ ($\sim 10\%$)

and laboratory, sediment slurry experiments ($\sim 9\%$). Anammox has only recently been reported in streambed sediments (Cheng et al. 2016; Han and Li 2016; Kim et al. 2016; Lansdown et al. 2016), largely due to the limited attempts to quantify it relative to the focus on denitrification. The similarity of results between in situ experiments and controlled laboratory experiments shows that the conditions in situ are close to optimal for anammox and that the push–pull method works well. This $\sim 10\%$ contribution of anammox to total nitrate reduction falls within the range measured across 9 other English lowland rivers (0–58%) and specifically, other work in permeable, sandy riverbeds also averaged 9% (Lansdown et al. 2016).

DNRA is similarly understudied in freshwater sediments principally because the techniques employed on many occasions in the past were either not capable of quantifying it directly (e.g. acetylene block) or were not sensitive enough (e.g. whole stream ^{15}N additions) or perhaps because DNRA recycles reactive nitrogen (into ammonium) rather than removing it from the system it has not been focus of previous work (Burgin and Hamilton 2007). DNRA contributed $\sim 5\%$ of the in situ total nitrate reduction in our study site (locally 0–63%). Studies which only report the bulk reduction in nitrate concentration (i.e. do not specifically quantify DNRA) are likely to over-estimate true inorganic-nitrogen removal from the system. The co-occurrence of anammox and DNRA can complicate the calculations as the latter could be providing ^{15}N -labelled ammonium as a substrate for the former (Nicholls and Trimmer 2009). However, the ambient ammonium pool is so large (average 161 μM) that even the highest rate of DNRA measured (371 nM N h^{-1}) only contributed 0.2% to this pool per hour and it is therefore unlikely to have significantly altered our anammox calculations.

Each in situ injection contained the same amount of nitrate, so the observed patterns reveal true differences in the potential for each process should nitrate penetrate the streambed. As these measurements were performed in situ, it is important to remember that the results of this study are influenced by mixing with the ambient pore water and the hydrology (i.e. water residence time). Further, the injected ^{15}N -nitrate was between 2 and 1300 times more concentrated than the ambient ^{14}N -nitrate pool, depending on location. Therefore, we are reporting in situ potentials for nitrate reduction as a function of large woody debris,

which could be higher than the true rate under ambient nitrate concentration.

Our pore water data indicate intense mineralisation of organic matter within the streambed through oxygen and nitrate, in the upper layers, and then through iron and, eventually, methanogenesis deeper down (Fig. 3, Table 1). Indeed, if we assume steady-state pore water profiles and Redfield ratios (106C:16 N:1P), approximately 50% of organic matter mineralisation terminated in methane e.g. mean CH_4 (507 μM)/mean NH_4^+ (161 μM) \times 6.6 (C:N) = \sim 50%. In more permeable, sandy-gravels [$\sim 10^{-10}$ to 10^{-9} m^2 (Huettel and Rusch 2000)] ammonium can accumulate at up to \sim 3 μM to 9 μM (Lansdown et al. 2014; Zarnetske et al. 2011), whereas here we measured appreciably more at up to 161 μM , which is more in line with similar, fine-sand sediments (Lansdown et al. 2016). With a median grain size of 258 μm , our fine-sand sediments have a lower permeability ($\sim 10^{-11}$ m^2 , Huettel and Rusch 2000) than sandy-gravels and solute exchange would be tending towards diffusion and, as a result, we see appreciable net accumulation of ammonium, methane and SRP. Despite this intense mineralisation, SRP was approximately half that expected for the concentration of ammonium. Again, assuming Redfield ratios (16:1), at 161 μM ammonium we would expect \sim 10 μM SRP but we measured far less at \sim 4 μM . Given that the sediments were rich in iron II (Table 1) some soluble phosphorus would have been precipitated with iron III complexes in the upper, oxidised layers (Froelich 1988; Sanders et al. 1997).

The influence of LWD on nitrate reduction

As highlighted by Krause et al. (2014), our mechanistic, system level understanding of the effectiveness of LWD in altering hydrological, geomorphological, thermal and biogeochemical processes in fine sediment dominated lowland streams is limited. This study has shown that the slower surface water velocities experienced in the observed lowland conditions reduce the impact of LWD on hydrodynamic forcing of surface water into the streambed in most instances, except where higher flow (e.g. February sampling period; Fig. 2c) results in increased hydraulic variation. This lack of LWD-induced forcing of surface water into the streambed and hyporheic zone, which

facilitate longer residence times and exposure of nitrate-rich sources to denitrification hot spots, limits the influence of LWD in enhancing nitrate reduction.

We found that the presence of LWD only had a direct influence on the rate of nitrate reduction in autumn, when river discharge was high. Nitrate concentrations were highest at locations around LWD, particularly during the autumn high flow event, indicating increased down-welling of nitrate-rich surface water into the streambed at locations $<$ 1 m away from LWD at high flow. This increased hyporheic exchange is likely due to enhanced surface water infiltration due to wood-induced bed-form complexity, as has been observed experimentally and in the field (Birgand et al. 2007; Elliott and Brooks 1997; Kail 2003; Klaar et al. 2011) and has been shown to be particularly effective at high discharge (Munz et al. 2011; Packman and Salehin 2003). Krause et al. (2014) predicted hyporheic residence times would be longer around LWD, due to fine sediment trapping around the wood structures. However, LWD didn't have such impact on the already fine sand dominated streambed characteristics at the field site, hence the opposite has been observed in our study; residence times were shorter in shallow sediments in close proximity to LWD, especially during high flow.

Previous research in nutrient poor upland streams revealed that hyporheic residence time (as a function of hyporheic exchange flow paths) was the dominant control of respiration and denitrification (Pinay et al. 1994; Zarnetske et al. 2011), where nitrate would be reduced when flow paths are long enough to ensure that high oxygen levels delivered by the surface water are depleted and sufficient organic carbon as an electron donor is still present to facilitate heterotrophic denitrification. For the lowland conditions observed in this study, the dominant fine grain size (average reach $D_{50} = 0.28$ mm), organic carbon rich streambed sediments and hypoxic pore-waters at the Hammer Stream caused immediate reduction of surface water born nitrate once it penetrated the streambed, meaning that surface water-born oxygen must have been respired in the top millimetres–centimetres of the streambed sediments.

Our results indicate that in lowland streams, simply allowing LWD to be recruited naturally may not provide significant increase in streambed roughness

and hyporheic exchange flow to facilitate enhanced nitrate attenuation. Engineered log-jams and instream wood restoration projects which are able to manipulate the size and complexity of LWD structures may assist in enhancing nitrate attenuation by increasing hyporheic exchange flow and residence times by increasing the hydrogeomorphic impact of LWD on the stream channel (Dixon 2016; Gippel 1995; Gippel et al. 1996; Hughes et al. 2008). However, as highlighted by (Craig et al. 2008), restoration efforts to enhance the ability of large streams (> 3rd order) to attenuate reactive nitrogen is difficult, and restoration efforts should be focused on smaller streams.

LWD is expected to have more substantial impacts on streambed nutrient spiralling in streambed environments that are not as rich in organic carbon and as strongly anoxic as in the investigated conditions of this study. In streams with higher pore water oxygen, the addition of LWD and associated fine sediment trapping may have a more pronounced effect. Additionally, the installation of engineered log jams designed to withstand high flow events and movement (particularly in highly mobile sandy streambeds such as this) which are embedded into the streambed and banks are likely to enhance hyporheic exchange flows and residence time at a range of flows, resulting in enhanced seasonal nitrate reduction. We therefore recommend that future wood restoration in lowland streams considers the physical manipulation of wood structures exceeding the dimensions of natural accumulations in this study to ensure that structures are designed in a manner which ensures hyporheic exchange flow and advective pumping are maximised, and that LWD is installed at locations where organic carbon may be limited.

Acknowledgements This work was funded by the Natural Environment Research Council (NE/L004437/1). We thank Liao Oulang, Louise Olde, Katrina Lansdown, Kris Hart, Victoria Warren and Ian Sanders for field assistance and Katrina Lansdown for technical support. We also acknowledge Curtis Horne for assistance with statistics.

Open Access This article is distributed under the terms of the Creative Commons Attribution 4.0 International License (<http://creativecommons.org/licenses/by/4.0/>), which permits unrestricted use, distribution, and reproduction in any medium, provided you give appropriate credit to the original author(s) and the source, provide a link to the Creative Commons license, and indicate if changes were made.

References

- Alexander RB, Smith RA, Schwarz GE (2000) Effect of stream channel size on the delivery of nitrogen to the Gulf of Mexico. *Nature* 403(6771):758–761
- Alexander RB, Boyer EW, Smith RA, Schwarz GE, Moore RB (2007) The role of headwater streams in downstream water quality. *JAWRA J Am Water Resour Assoc* 43(1):41–59
- Aumen NG, Hawkins CP, Gregory SV (1990) Influence of woody debris on nutrient retention in catastrophically disturbed streams. *Hydrobiologia* 190(3):183–192
- Barton K (2016) MuMIn: multi-model inference. In: 1.15.6 Rpv (ed)
- Bates D, Maechler M, Bolker B, Walker S (2015) Fitting linear mixed-effects models using lme4. *J Stat Softw* 67(1):1–48
- Benstead JP, Leigh DS (2012) An expanded role for river networks. *Nature Geosci* 5(10):678–679
- Bernhardt ES, Likens GE, Hall RO, Buso DC, Fisher SG, Burton TM, Meyer JL, McDowell WH, Mayer MS, Bowden WB, Findlay SEG, Macneale KH, Stelzer RS, Lowe WH (2005) Can't see the forest for the stream? In-stream processing and terrestrial nitrogen exports. *Bioscience* 55(3):219–230
- Bernot MJ, Dodds WK (2005) Nitrogen retention, removal, and saturation in lotic ecosystems. *Ecosystems* 8(4):442–453
- Birgand F, Skaggs RW, Chescheir GM, Gilliam JW (2007) Nitrogen removal in streams of agricultural catchments—a literature review. *Crit Rev Environ Sci Technol* 37(5):381–487
- Bouraoui F, Grizzetti B (2011) Long term change of nutrient concentrations of rivers discharging in European seas. *Sci Total Environ* 409(23):4899–4916
- Burgin AJ, Hamilton SK (2007) Have we overemphasized the role of denitrification in aquatic ecosystems? A review of nitrate removal pathways. *Front Ecol Environ* 5(2):89–96
- Burnham KP, Anderson DR (2004) Multimodel Inference. *Sociol Methods Res* 33(2):261–304
- Burt T, Howden N, Worrall F, Whelan M (2008) Importance of long-term monitoring for detecting environmental change: lessons from a lowland river in south east England. *Bio-geosciences* 5(6):1529–1535
- Camargo JA, Alonso Á (2006) Ecological and toxicological effects of inorganic nitrogen pollution in aquatic ecosystems: a global assessment. *Environ Int* 32(6):831–849
- Canfield DE, Glazer AN, Falkowski PG (2010) The evolution and future of Earth's nitrogen cycle. *Science* 330(6001):192–196
- Cheng L, Li XF, Lin XB, Hou LJ, Liu M, Li Y, Liu S, Hu XT (2016) Dissimilatory nitrate reduction processes in sediments of urban river networks: Spatiotemporal variations and environmental implications. *Environ Pollut* 219:545–554
- Craig LS, Palmer MA, Richardson DC, Filoso S, Bernhardt ES, Bledsoe BP, Doyle MW, Groffman PM, Hassett BA, Kaushal SS, Mayer PM, Smith SM, Wilcock PR (2008) Stream restoration strategies for reducing river nitrogen loads. *Front Ecol Environ* 6(10):529–538
- Curran JH, Wohl EE (2003) Large woody debris and flow resistance in step-pool channels, Cascade Range, Washington. *Geomorphology* 51(1):141–157
- Dixon SJ (2016) A dimensionless statistical analysis of logjam form and process. *Ecology* 9(6):1117–1129

- Dodds WK, Oakes RM (2008) Headwater influences on downstream water quality. *Environ Manag* 41(3):367–377
- Eaton AD, Clesceri LS, Rice EW, Greenberg AE (2005) APHA-AWWA-WPCF standard methods for the examination of water and wastewater. American Public Health Association, Washington, DC
- Elliott AH, Brooks NH (1997) Transfer of nonsorbing solutes to a streambed with bed forms: Theory. *Water Resour Res* 33(1):123–136
- Elosegi A, Elorriaga C, Flores L, Martí E, Díez J (2016) Restoration of wood loading has mixed effects on water, nutrient, and leaf retention in Basque mountain streams. *Freshw Sci* 35(1):41–54
- Erismann JW, Galloway JN, Seitzinger S, Bleeker A, Dise NB, Petrescu AR, Leach AM, de Vries W (2013) Consequences of human modification of the global nitrogen cycle. *Philos Trans R Soc B* 368(1621):20130116
- Filoso S, Palmer MA (2011) Assessing stream restoration effectiveness at reducing nitrogen export to downstream waters. *Ecol Appl* 21(6):1989–2006
- Fox J, Weisberg S (2011) An {R} Companion to Applied Regression. In: Sage, Thousand Oaks (CA)
- Froelich PN (1988) Kinetic control of dissolved phosphate in natural rivers and estuaries: a primer on the phosphate buffer mechanism I. *Limnol Oceanogr* 33(4 (Part 2)):649–668
- Gippel CJ (1995) Environmental hydraulics of large woody debris in streams and rivers. *J Environ Eng* 121(5):388–395
- Gippel CJ, O'Neill I, Finlayson BL, Schnatz I (1996) Hydraulic guidelines for the re-introduction and management of large woody debris in lowland rivers. *Regul Rivers Res Manag* 12(23):223–236
- Godfray HCJ, Garnett T (2014) Food security and sustainable intensification. *Philos Trans R Soc B* 369(1639):20120273
- Gomez-Velez JD, Harvey JW, Cardenas MB, Kiel B (2015) Denitrification in the Mississippi River network controlled by flow through river bedforms. *Nat Geosci* 8:941–945
- Gruber N, Galloway JN (2008) An Earth-system perspective of the global nitrogen cycle. *Nature* 451(7176):293–296
- Gurnell AM, Gregory KJ, Petts GE (1995) The role of coarse woody debris in forest aquatic habitats: implications for management. *Aquat Conserv Mar Freshw Ecosyst* 5(2):143–166
- Han HY, Li ZK (2016) Effects of macrophyte-associated nitrogen cycling bacteria on ANAMMOX and denitrification in river sediments in the Taihu Lake region of China. *Ecol Eng* 93:82–90
- Howarth RW (2008) Coastal nitrogen pollution: a review of sources and trends globally and regionally. *Harmful Algae* 8(1):14–20
- Howden NJ, Burt TP, Worrall F, Mathias SA, Whelan MJ (2013) Farming for water quality: balancing food security and nitrate pollution in UK river basins. *Ann Assoc Am Geogr* 103(2):397–407
- Huettel M, Rusch A (2000) Transport and degradation of phytoplankton in permeable sediment. *Limnol Oceanogr* 45(3):534–549
- Hughes V, Thoms MC, Nicol S, Koehn J (2008) Physical-ecological interactions in a lowland river system: large wood, hydraulic complexity and native fish associations in the River Murray, Australia. In: Wood PJ, Hannah DM, Sadler JP (eds) *Hydrecology and ecohydrology: past, present, and future*. Wiley, Chichester, pp 387–404
- Kail J (2003) Influence of large woody debris on the morphology of six central European streams. *Geomorphology* 51(1):207–223
- Kasahara T, Datry T, Mutz M, Boulton AJ (2009) Treating causes not symptoms: restoration of surface-groundwater interactions in rivers. *Mar Freshw Res* 60(9):976–981
- Keller EA, Swanson FJ (1979) Effects of large organic material on channel form and fluvial processes. *Earth Surf Process* 4(4):361–380
- Kim H, Bae HS, Reddy KR, Ogram A (2016) Distributions, abundances and activities of microbes associated with the nitrogen cycle in riparian and stream sediments of a river tributary. *Water Res* 106:51–61
- Kirkwood D (1996) Nutrients: practical notes on their determination in sea water. *Mar Environ Sci* 17:1–25
- Klaar MJ, Hill DF, Maddock I, Milner AM (2011) Interactions between instream wood and hydrogeomorphic development within recently deglaciated streams in Glacier Bay National Park, Alaska. *Geomorphology* 130(3):208–220
- Krause S, Heathwaite L, Binley A, Keenan P (2009) Nitrate concentration changes at the groundwater-surface water interface of a small Cumbrian river. *Hydrol Process* 23(15):2195–2211
- Krause S, Tecklenburg C, Munz M, Naden E (2013) Streambed nitrogen cycling beyond the hyporheic zone: flow controls on horizontal patterns and depth distribution of nitrate and dissolved oxygen in the upwelling groundwater of a lowland river. *J Geophys Res Biogeosci* 118(1):54–67
- Krause S, Klaar M, Hannah D, Mant J, Bridgeman J, Trimmer M, Manning-Jones S (2014) The potential of large woody debris to alter biogeochemical processes and ecosystem services in lowland rivers. *Wiley Interdiscip Rev Water* 1(3):263–275
- Lansdown K, Trimmer M, Heppell C, Sgouridis F, Ullah S, Heathwaite A, Binley A, Zhang H (2012) Characterization of the key pathways of dissimilatory nitrate reduction and their response to complex organic substrates in hyporheic sediments. *Limnol Oceanogr* 57(2):387–400
- Lansdown K, Heppell CM, Dossena M, Ullah S, Heathwaite AL, Binley A, Zhang H, Trimmer M (2014) Fine-scale in situ measurement of riverbed nitrate production and consumption in an armored permeable riverbed. *Environ Sci Technol* 48(8):4425–4434
- Lansdown K, McKew B, Whitby C, Heppell C, Dumbrell A, Binley A, Olde L, Trimmer M (2016) Importance and controls of anaerobic ammonium oxidation influenced by riverbed geology. *Nat Geosci* 9(5):357–360
- McClain EM, Boyer WE, Dent LC, Gergel ES, Grimm BN, Groffman MP, Hart CS, Harvey WJ, Johnston AC, Mayorga E, McDowell HW, Pinay G (2003) Biogeochemical Hot Spots and Hot Moments at the Interface of Terrestrial and Aquatic Ecosystems. *Ecosystems* 6(4):301–312
- McIsaac GF, David MB, Gertner GZ, Goolsby DA (2001) Eutrophication: nitrate flux in the Mississippi River. *Nature* 414(6860):166–167
- Miller SW, Budy P, Schmidt JC (2010) Quantifying macroinvertebrate responses to in-stream habitat restoration: applications of meta-analysis to river restoration. *Restor Ecol* 18(1):8–19

- Mulholland PJ, Helton AM, Poole GC, Hall RO, Hamilton SK, Peterson BJ, Tank JL, Ashkenas LR, Cooper LW, Dahm CN (2008) Stream denitrification across biomes and its response to anthropogenic nitrate loading. *Nature* 452(7184):202–205
- Munz M, Krause S, Tecklenburg C, Binley A (2011) Reducing monitoring gaps at the aquifer–river interface by modelling groundwater–surface water exchange flow patterns. *Hydrol Process* 25(23):3547–3562
- Nicholls JC, Trimmer M (2009) Widespread occurrence of the anammox reaction in estuarine sediments. *Aquat Microb Ecol* 55(2):105–113
- Packman AI, Salehin M (2003) Relative roles of stream flow and sedimentary conditions in controlling hyporheic exchange. In: Kronvang B (ed) *The interactions between sediments and water*. Springer, New York, pp 291–297
- Peterson BJ, Wollheim WM, Mulholland PJ, Webster JR, Meyer JL, Tank JL, Marti E, Bowden WB, Valett HM, Hershey AE, McDowell WH, Dodds WK, Hamilton SK, Gregory S, Morrall DD (2001) Control of nitrogen export from watersheds by headwater streams. *Science* 292(5514):86–90
- Pinay G, Haycock N, Ruffioni C, Holmes R (1994) The role of denitrification in nitrogen retention in river corridors. In: Mitsch WJ (ed) *Global wetlands: old world and new*. Elsevier, Amsterdam
- Pinay G, Peiffer S, De Dreuzy J-R, Krause S, Hannah DM, Fleckenstein JH, Sebilo M, Bishop K, Hubert-Moy L (2015) Upscaling nitrogen removal capacity from local hotspots to low stream orders' drainage basins. *Ecosystems* 18(6):1101–1120
- Pinheiro J, Bates D, DebRoy S, Sarkar D (2014) NLME: Linear and nonlinear mixed effects models. R Package Version 3, 1–117
- Powlson DS, Addiscott TM, Benjamin N, Cassman KG, de Kok TM, van Grinsven H, L'hirondel J-L, Avery AA, van Kessel C (2008) When does nitrate become a risk for humans? *J Environ Qual* 37(2):291–295
- R Core Team (2015) R: a language and environment for statistical computing. The R Foundation for Statistical Computing, Vienna
- Richardson WB, Strauss EA, Bartsch LA, Monroe EM, Cavanaugh JC, Vingum L, Soballe DM (2004) Denitrification in the Upper Mississippi River: rates, controls, and contribution to nitrate flux. *Can J Fish Aquat Sci* 61(7):1102–1112
- Risgaard-Petersen N, Revsbech NP, Rysgaard S (1995) Combined microdiffusion-hypobromite oxidation method for determining nitrogen-15 isotope in ammonium. *Soil Sci Soc Am J* 59(4):1077–1080
- Risgaard-Petersen N, Meyer RL, Schmid M, Jetten MS, Enrich-Prast A, Rysgaard S, Revsbech NP (2004) Anaerobic ammonium oxidation in an estuarine sediment. *Aquat Microb Ecol* 36:293–304
- Rivett M, Ellis P, Greswell R, Ward R, Roche R, Cleverly M, Walker C, Conran D, Fitzgerald P, Willcox T (2008) Cost-effective mini drive-point piezometers and multilevel samplers for monitoring the hyporheic zone. *Q J Eng Geol Hydrogeol* 41(1):49–60
- Roberts BJ, Mulholland PJ, Houser JN (2007) Effects of upland disturbance and instream restoration on hydrodynamics and ammonium uptake in headwater streams. *J N Am Benthol Soc* 26(1):38–53
- Sanders RJ, Jickells T, Malcolm S, Brown J, Kirkwood D, Reeve A, Taylor J, Horrobin T, Ashcroft C (1997) Nutrient fluxes through the Humber estuary. *J Sea Res* 37(1):3–23
- Sanders IA, Heppell CM, Cotton JA, Wharton G, Hildrew AG, Flowers EJ, Trimmer M (2007) Emission of methane from chalk streams has potential implications for agricultural practices. *Freshw Biol* 52(6):1176–1186
- Schlesinger WH (2009) On the fate of anthropogenic nitrogen. *Proc Natl Acad Sci* 106(1):203–208
- Seitzinger SP (1988) Denitrification in freshwater and coastal marine ecosystems: ecological and geochemical significance. *Limnol Oceanogr* 33(4 (part 2)):702–724
- Seitzinger SP, Styles RV, Boyer EW, Alexander RB, Billen G, Howarth RW, Mayer B, van Breemen N (2002) Nitrogen retention in rivers: model development and application to watersheds in the northeastern USA. *Biogeochemistry* 57(1):199–237
- Shrimali M, Singh KP (2001) New methods of nitrate removal from water. *Environ Pollut* 112(3):351–359
- Smart RM, Barko JW (1985) Laboratory culture of submersed freshwater macrophytes on natural sediments. *Aquat Bot* 21(3):251–263
- Survey BG (2016) <http://mapapps.bgs.ac.uk/geologyofbritain/home.html>. In: vol 22nd September
- Sylvester-Bradley R, Kindred DR (2009) Analysing nitrogen responses of cereals to prioritize routes to the improvement of nitrogen use efficiency. *J Exp Bot* 60(7):1939–1951
- Thamdrup B, Dalsgaard T (2000) The fate of ammonium in anoxic manganese oxide-rich marine sediment. *Geochim Cosmochim Acta* 64(24):4157–4164
- Thamdrup B, Dalsgaard T, Jensen MM, Ulloa O, Farías L, Escribano R (2006) Anaerobic ammonium oxidation in the oxygen-deficient waters off northern Chile. *Limnol Oceanogr* 51(5):2145–2156
- Trimmer M, Risgaard-Petersen N, Nicholls JC, Engström P (2006) Direct measurement of anaerobic ammonium oxidation (anammox) and denitrification in intact sediment cores. *Mar Ecol Prog Ser* 326:37–47
- Trimmer M, Grey J, Heppell CM, Hildrew AG, Lansdown K, Stahl H, Yvon-Durocher G (2012) River bed carbon and nitrogen cycling: state of play and some new directions. *Sci Total Environ* 434:143–158
- Van de Graaf AA, de Bruijn P, Robertson LA, Jetten MS, Kuenen JG (1996) Autotrophic growth of anaerobic ammonium-oxidizing micro-organisms in a fluidized bed reactor. *Microbiology* 142(8):2187–2196
- Warren DR, Judd KE, Bade DL, Likens GE, Kraft CE (2013) Effects of wood removal on stream habitat and nitrate uptake in two northeastern US headwater streams. *Hydrobiologia* 717(1):119–131
- Webster J, Tank J, Wallace J, Meyer J, Eggert S, Ehrman T, Ward B, Bennett B, Wagner P, McTammany M (2000) Effects of litter exclusion and wood removal on phosphorus and nitrogen retention in a forest stream. *Verh Int Verein Limnol* 27:1337–1340
- Weiss R, Price B (1980) Nitrous oxide solubility in water and seawater. *Mar Chem* 8(4):347–359
- Yamamoto S, Alcauskas JB, Crozier TE (1976) Solubility of methane in distilled water and seawater. *J Chem Eng Data* 21(1):78–80

Zarnetske JP, Haggerty R, Wondzell SM, Baker MA (2011) Dynamics of nitrate production and removal as a function of residence time in the hyporheic zone. *J Geophys Res Biogeosci.* <https://doi.org/10.1029/2010JG001356>

Zhou S, Borjigin S, Riya S, Terada A, Hosomi M (2014) The relationship between anammox and denitrification in the sediment of an inland river. *Sci Total Environ* 490:1029–1036